Nesprin-3, a novel outer nuclear membrane protein, associates with the cytoskeletal linker protein plectin

Kevin Wilhelmsen, Sandy H.M. Litjens, Ingrid Kuikman, Ntambua Tshimbalanga, Hans Janssen, Iman van den Bout, Karine Raymond, and Arnoud Sonnenberg

Division of Cell Biology, Netherlands Cancer Institute, 1066 CX Amsterdam, Netherlands

Despite their importance in cell biology, the mechanisms that maintain the nucleus in its proper position in the cell are not well understood. This is primarily the result of an incomplete knowledge of the proteins in the outer nuclear membrane (ONM) that are able to associate with the different cytoskeletal systems. Two related ONM proteins, nuclear envelope spectrin repeat (nesprin)–1 and –2, are known to make direct connections with the actin cytoskeleton through their NH_2-terminal actin-binding domain (ABD). We have now isolated a third member of the nesprin family that lacks an ABD and instead binds to the plakin family member plectin, which can associate with the intermediate filament (IF) system. Overexpression of nesprin-3 results in a dramatic recruitment of plectin to the nuclear perimeter, which is where these two molecules are colocalized with both keratin-6 and -14. Importantly, plectin binds to the integrin $\alpha6\beta4$ at the cell surface and to nesprin-3 at the ONM in keratinocytes, suggesting that there is a continuous connection between the nucleus and the extracellular matrix through the IF cytoskeleton.

Introduction

The three cytoskeletal filament systems of eukaryotic cells are composed of actin filaments, intermediate filaments (IFs), and microtubules (MTs). They are responsible for such diverse functions as the transport and positioning of organelles in the cytoplasm, the segregation of the chromosomes during mitosis, cell shape, cell movement, and the structural integrity of the membranes (Fuchs and Karakesisoglou, 2001). The three systems are connected to each other through the members of the plakin family of cytoskeletal cross-linkers (Sun et al., 2001; Jefferson et al., 2004). Three members of this family are the bullous pemphigoid antigen-1 (BPAG1), the MT–actin cross-linking factor (MACF), and plectin. MACF is primarily responsible for cross-linking the actin filaments and MTs (Sun et al., 2001), whereas plectin can directly cross-link the actin and IF cytoskeletal systems (Wiche, 1998). In BPAG1, there are several different tissue-specific splice variants that are capable of cross-linking the actin and MT systems (Leung et al., 2001). These molecules are very large (834 [BPAG1b], 520 [plectin], and 608 kD [MACF]) and the binding domains for the different cytoskeletal systems are on opposite ends of the proteins, which may allow for a physiologically important spacing between the different structural systems.

Plakins can also mediate the binding of the cytoskeleton to membrane-bound protein complexes within a cell (Fuchs and Karakesisoglou, 2001). The NH_2-terminal sequences of the 11 known plectin isoforms, which result from alternative splicing, are important for the cytoplasmic localization of these molecules (Fuchs et al., 1999; Rezniczek et al., 2003). For example, the actin-binding domain (ABD) of plectin-1A and -1C can bind to the cytoplasmic domain of the integrin β4 subunit at the plasma membrane to initiate the formation of hemidesmosomes, which are adhesion structures that allow for the firm attachment of the basal epithelial cells to the underlying basement membrane (Borradori and Sonnenberg, 1999; Koster et al., 2004a). In addition, plectin-1F can become localized at focal contacts (FCs), whereas plectin-1B is associated with proteins of the mitochondria (Rezniczek et al., 2003). The binding properties of the latter two isoforms suggest that plectin can mediate the linkage of the IF system to proteins in lipid bilay-

K. Wilhelmsen and S.H.M. Litjens contributed equally to this paper.

Correspondence to Arnoud Sonnenberg: a.sonnenberg@nki.nl

Abbreviations used in this paper: ABD, actin-binding domain; BPAG1, bullous pemphigoid antigen-1; cDNA, complementary DNA; EBS-MD, epidermolysis bullosa simplex with muscular dystrophy; FC, focal contact; FNIII, fibronectin type III; IF, intermediate filament; INM, inner nuclear membrane; KASH, Klarsicht/ANC-1/Syne-1 homology; MACF, MT–actin cross-linking factor; MEF, mouse embryonic fibroblast; MT, microtubule; NE, nuclear envelope; nesprin, nuclear envelope spectrin repeat; ONM, outer nuclear membrane; pAb, polyclonal antibody; PA-JEB, pyloric atresia associated with junctional epidermolysis bullosa; RACE, rapid analysis of cDNA ends; mRFP, monomeric red fluorescent protein; RIPA, radioimmunoprecipitation; siRNA, small interfering RNA; SMART, simple modular architecture research tool; SR, spectrin repeat; TM, transmembrane domain; VSV, vesicular stomatitis virus; WCL, whole cell lysate; Y2H, yeast two-hybrid.

The online version of this paper contains supplemental material.

The Journal of Cell Biology, Vol. 171, No. 5, December 5, 2005 799–810
http://www.jcb.org/cgi/doi/10.1083/jcb.200506083

ers other than those of the plasma membrane. BPAG1-e (also known as BP230) also links the IF cytoskeleton to hemidesmosomes, and there is evidence that BPAG1 can associate with transmembrane glycoproteins on the plasma membrane (Guo et al., 1995; Hopkinson and Jones, 2000; Nakayama et al., 2002; Koster et al., 2003). MACF, on the other hand, has been reported to be localized at the plasma membrane at cell–cell contacts and, recently, to membranes of the Golgi apparatus (Karakesisoglou et al., 2000; Kakinuma et al., 2004; Lin et al., 2005). Together, the evidence shows that the plakin family members, in addition to their role as cross-linkers of the cytoskeleton, can form a bridge between membrane-bound proteins and the various cytoskeletal systems. However, no plakin family members have been reported to associate with proteins of the nuclear envelope (NE).

The NE separates the nucleoplasm from the cytoplasm and consists of two lipid bilayers, the inner nuclear membrane (INM) and the outer nuclear membrane (ONM). The INM contains a distinctive set of integral membrane proteins that interact with chromatin through associated proteins such as the nuclear lamins, which is a meshwork of IF proteins that underlies the INM (Burke and Stewart, 2002). Lamins themselves can also bind chromatin and play an essential role in maintaining the structural integrity of the NE (Hutchison, 2002; Gruenbaum et al., 2005). The proper position of the nucleus in a cell is thought to be maintained through the linkage of ONM proteins to the different cytoskeletal systems. In vertebrates, the only ONM proteins known to make associations with the cytoskeleton are the related integral membrane proteins NE spectrin repeat (nesprin)–1 and –2, which bind to actin through their NH_2-terminal ABDs (Zhang et al., 2002). However, in *Caenorhabditis elegans*, UNC-83 can link the nucleus to the MT cytoskeleton (Starr et al., 2001). This suggests that in higher organisms there are ONM proteins that can link the nucleus not only to the actin cytoskeleton but also to MTs.

The type II ONM proteins nesprin-1 and -2 (also known as Myne-1 and -2; Mislow et al., 2002), Syne-1 and -2 (Apel et al., 2000), or Enaptin and Nuance (Zhen et al., 2002; Padmakumar et al., 2004) contain a central rod domain with a variable number of spectrin repeats (SRs), flanked by an NH_2-terminal ABD and a conserved COOH-terminal domain (Zhang et al., 2001, 2002). The NH_2-terminal ABD is of the type found in β-spectrin and consists of two calponin homology domains. The conserved COOH-terminal domain, which includes the transmembrane domain (TM) and the COOH-terminal amino acids present in the periplasmic space of the NE, shares a homologous region with the *Drosophila melanogaster* protein Klarsicht and is therefore referred to as the Klarsicht/ANC-1/Syne-1 homology (KASH) or Klarsicht-like domain. However, apart from this domain there are no other features shared with the *D. melanogaster* protein (Mosley-Bishop et al., 1999). In humans, both nesprin-1 and -2 are giant proteins with molecular masses of ∼976 and 764 kD, respectively. Because of the presence of an ABD, it has been suggested that nesprins play an important role in nuclear positioning. Indeed, the single homologue of nesprin in *C. elegans*, ANC-1, is required for the proper anchorage of nuclei to actin in syncytial cells (Starr and Han, 2002, 2003) and recently, overexpression of the KASH domain in mice highlighted the importance of Syne-1 for the proper positioning and localization of synaptic nuclei (Grady et al., 2005).

		nesprin-related Y2H sequence	first Pair β4-FNIII domains
	plectin-1C	+	+
76%	BPAG1-n	+	+
52%	α-actinin-1	-	-
47%	dystrophin	-	-
34%	filamin-B	-	-
31%	filamin-A	-	-

Figure 1. **Y2H analysis of the interaction between either the nesprin-related Y2H sequence or the first pair of FNIII domains of β4 with several different ABDs.** Interactions were scored + when the plating efficiencies on selective SC-LTHA plates were >30% of those on nonselective SC-LT plates at 5 d of growth. Interactions were scored − when no colonies were detected at 10 d of growth. The percent homology of the other ABDs to the plectin ABD is shown in the column on the left. The results for the interactions of the first pair of FNIII domains with the ABDs listed have been reported previously (Litjens et al., 2003).

We have identified a new member of the nesprin family that can bind to the plakin family member plectin at the ONM. This protein was isolated in a yeast two-hybrid (Y2H) screen using the ABD of plectin-1C as bait. Like the other two known nesprins, nesprin-3 is a type II transmembrane protein of the ONM and contains a COOH-terminal KASH domain and a series of SRs related to those in nesprin-1 and -2. Unlike the other two full-length nesprins, nesprin-3 lacks an ABD and is therefore not able to associate with actin, but instead may associate with the IF cytoskeleton through plectin. Nesprin-3 is ubiquitously expressed in all cell lines and tissues tested. Expression of nesprin-3 strongly recruited endogenous plectin to the ONM in cells, where it was colocalized with both keratin-6 and -14 filaments. Nesprin-3 is the first ONM protein with an established link to the IF cytoskeletal system, and it seems certain that its discovery will increase our knowledge of the function of the NE during mitosis and proper nuclear positioning during quiescence and cell migration.

Results

Identification of a novel protein that interacts with the plectin ABD

It is well documented that the integrin β4 subunit is bound to plectin in hemidesmosomes (Borradori and Sonnenberg, 1999). We have shown previously that the critical binding site between plectin and β4 occurs through the first pair of fibronectin type III (FNIII) domains of β4 and the NH_2-terminal ABD of plectin (Geerts et al., 1999; Litjens et al., 2003; Koster et al., 2004b). We were curious to find out if additional proteins could bind to the plectin ABD. For this purpose, we performed a Y2H genetic screen using the human plectin-1C ABD as bait. We identified several novel interactions with both known and previously unidentified proteins. Of the unknown proteins, one showed homology with the related type II ONM proteins, nesprin-1 and -2. We then tested the ability of the nesprin-related

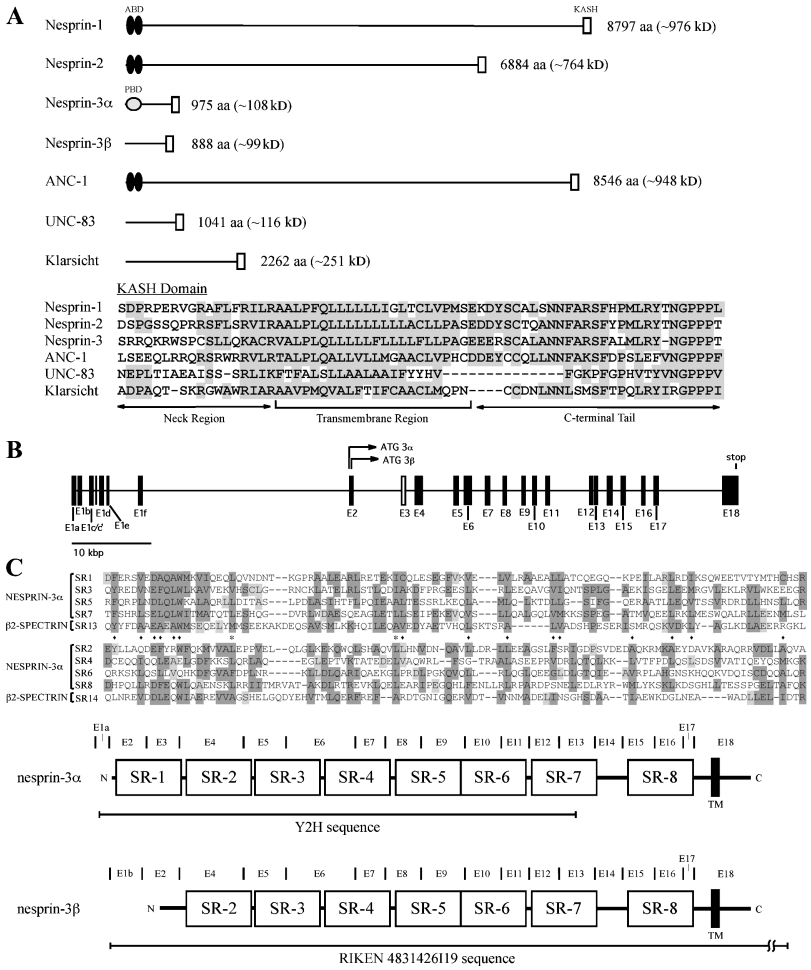

Figure 2. **Sequence analysis of nesprin-3.** (A) Scaled diagrams of the nesprin-1, -2, -3α, and -3β, ANC-1, UNC-83, and *D. melanogaster* Klarsicht protein are presented. The sequence alignment of the KASH domain of the different murine nesprins, ANC-1 and UNC-83, with the conserved domain in the *D. melanogaster* Klarsicht protein is shown with similar amino acids shaded gray. (B) Organization of the nesprin-3 genome. The 18 exons are labeled as E1–E18 and are depicted as closed bars, except the exon unique to nesprin-3α (E3), which is depicted as an open box. The translation start sites for nesprin-3α and -3β are shown in E2. The distances are drawn to scale with the measurement bar. (C) SRs 1, 3, 5, and 7, and 2, 4, 6, and 8 of nesprin-3α are shown aligned with the 13th and 14th SRs of spectrin-β2, respectively. Dark gray boxes depict alignment of more than three similar amino acids in an alignment set. Light gray boxes depict similar amino acids to a majority of those in the opposing alignment set. A diamond indicates that residues are conserved in only one alignment set, and an asterisk indicates residues that are conserved in both sets. Below the SR alignment the structures of nesprin-3α and -3β are shown. The location of the exons are denoted by bars and labeled in between each accordingly as E1–E18. The region of nesprin-3α encoded by the cDNA found in the Y2H screen is underlined, as is the sequence for nesprin-3β (RIKEN clone 4831426I19) found in the database. The SRs are depicted as open boxes. In exon 18, the RIKEN sequence continues for another 2,198 nucleotides after the stop codon. The NH_2 terminus is to the left and the COOH terminus is to the right. The distances are drawn to scale.

protein sequence to bind to other ABDs in a Y2H assay, using the previously published results for the first pair of FNIII domains of β4 to bind the same ABDs as a control (Litjens et al., 2003). The results show that, like β4, the nesprin-related sequence binds to the plectin-1C ABD and the BPAG1-n ABD, which is highly homologous to the plectin ABD (76% homology). However, the nesprin-related protein sequence, also like β4, did not bind to the ABDs of dystrophin, α-actinin-1, and filamin-A and -B (Fig. 1). We conclude that the nesprin-related sequence has the same binding specificity as the β4 subunit for the different ABDs.

Genomic organization of nesprin-3

A basic local alignment search tool search with the novel plectin-1C ABD binding sequence showed stretches of nucleotide sequences identical with an Institute of Physical and Chemical Research (RIKEN) complementary DNA (cDNA; 4831426I19) and homology to a region in nesprin-1 and -2 containing a variable number of SRs. In the mouse genome, the nesprin-1 gene is on chromosome 10A1 (human homologue 6q25) and the nesprin-2 gene is on chromosome 12C3 (human homologue 14q23.2). Software analysis revealed that the gene for the novel nesprin-related sequence is also on chromosome 12, but in a different location than nesprin-2, in region 12E (human homologue 14q32.13, showing 72% homology). Database searches revealed that the cDNA for the nesprin-related protein sequence is also present in cDNA libraries of several other species, including the rat, chimpanzee, dog, and chicken (68, 68, 50, and 43% homology, respectively). Furthermore, the RIKEN clone contained a COOH-terminal KASH domain that was similar to that found in nesprin-1 and -2 (51 and 61% protein sequence homology, respectively; Fig. 2 A). These database analyses indicate that the nesprin-related cDNA sequence encodes a novel nesprin family member, which will be referred to as nesprin-3.

Comparison of the RIKEN cDNA 4831426I19 and the nesprin-3 Y2H nucleotide sequences with the mouse genomic sequence on chromosome 12 revealed that these two ORFs represent splice variants of the nesprin-3 gene because we identified alternatively spliced exon 1 sequences for the Y2H and RIKEN sequences, labeled exons 1a and 1b, respectively, and an additional 173-nucleotide exon in the Y2H sequence (exon 3; Fig. 2 B and Fig. S1, A and B, available at http://www.jcb.org/cgi/content/full/jcb.200506083/DC1). Additionally, both sequences contain an identical exon 2, but the reading frame is different in this exon for the two nesprin-3 splice variants; therefore, these proteins have different NH_2-terminal sequences (Fig. S1 A). RT-PCR analysis on total mRNA from several cell lines suggests that after exon 3 the nucleotide (and protein) sequence is the same in the two splice variants and is

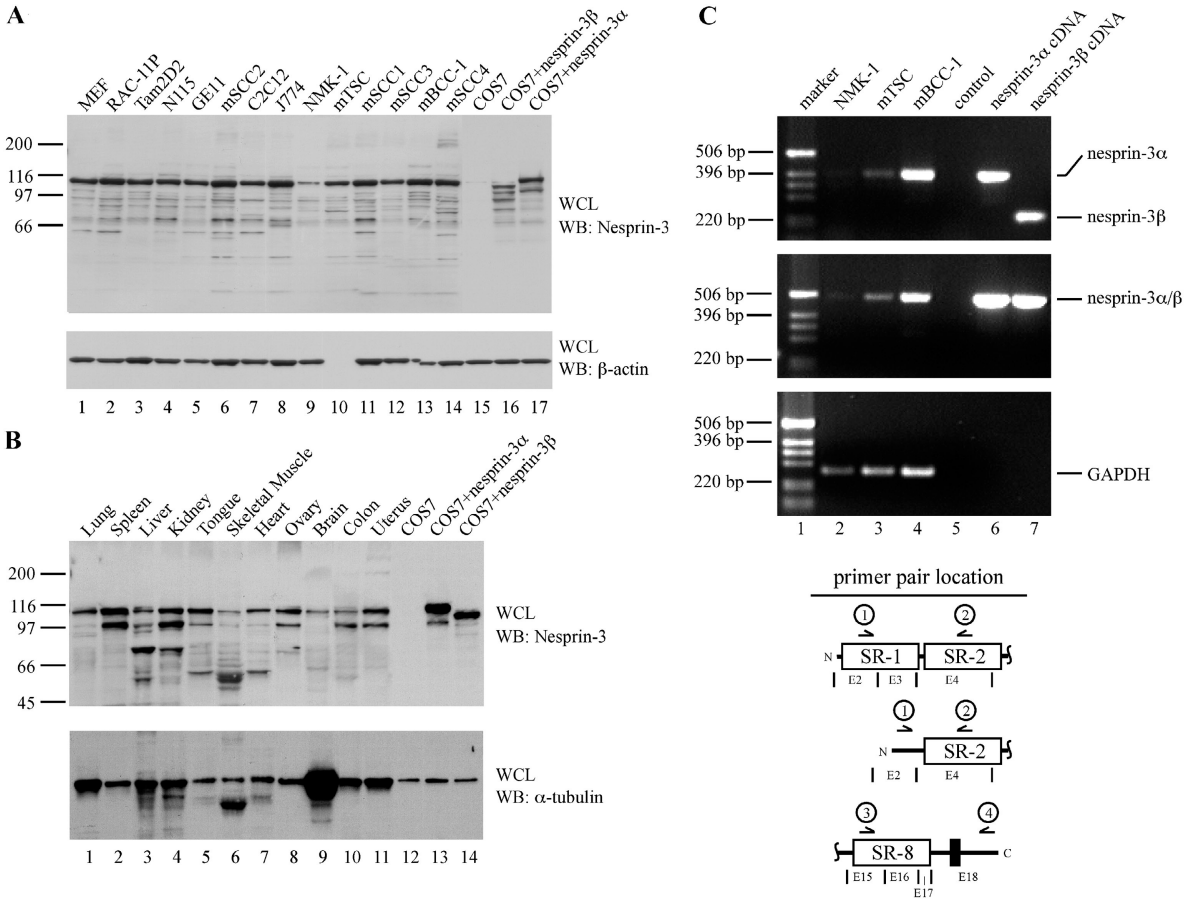

Figure 3. **Tissue and cell line distribution of nesprin-3.** (A) The indicated mouse-derived cell lines were lysed with RIPA buffer to extract NE components. Whole cell lysates (WCLs) of untransfected, nesprin-3α cDNA–transfected, or nesprin-3β cDNA–transfected COS7 cells were included as controls. WCL samples were loaded and run in a 4–20% SDS-PAGE gel, transferred to PVDF membrane, and probed for the presence of nesprin-3 using the GST-nesprin-3-SR7–derived antibodies. A protein blot for β-actin was used as a loading control. (B) The indicated mouse tissues were dounce homogenized in RIPA buffer. WCLs of these samples were analyzed as in B. A protein blot for α-tubulin was used as a loading control. (C) To determine the selectivity of nesprin-3α and -3β expression, the mouse cell lines NMK-1, mTSC, and mBCC-1 were used. Primers annealing on either side of the nesprin-3α–specific exon 3 (primers 1 and 2) were used to determine the presence of either variant in these cell lines (top; see Results). Primers that would amplify exons 15–18 of nesprin-3 (primers 3 and 4) were used as a control for mRNA fidelity and specificity (middle). Nesprin-3α and -3β cDNAs were used as controls in these PCR reactions. A PCR of GAPDH was also included as a control for nesprin-3 expression levels and mRNA fidelity (bottom). Schematic representations (Fig. 2 C) of the regions of nesprin-3α and -3β amplified by primer pairs are shown underneath the image. Only part of nesprin-3 is depicted, for simplicity.

encoded by exons 4–18 (Fig. 2 B, Fig. 3 C, and Fig. S1 A). Because the nesprin-3 Y2H sequence was the originally discovered sequence and may represent a longer nesprin-3 variant, we will now refer to this variant as nesprin-3α, whereas the RIKEN cDNA–encoded polypeptide will be referred to as nesprin-3β.

Using the simple modular architecture research tool (SMART) motif scanning software, we identified several SRs in nesprin-3. The protein sequence showed 25% homology with the same region in both mouse and human nesprin-1 and 22% homology with the same region in human nesprin-2. Manual inspection of the nesprin-3α cDNA sequence showed the presence of eight related SRs, some of which were not recognized by the SMART software (Fig. 2 C and Fig. S1 A). The first SR is encoded by the nesprin-3α alternative reading frame in exon 2 and the nesprin-3α–specific exon 3. Therefore, nesprin-3β does not have the first SR, but does contain SRs 2–8 (Fig. 2 C and Fig. S1 A).

To determine if longer variants of nesprin-3 exist, we performed 5′–rapid analysis of cDNA ends (RACE) analysis on mRNA from the Rac-11P and mTSC cell lines. The results indicate that the original nesprin-3 Y2H sequence contains the true start site of translation for nesprin-3α because the longest transcript detected containing exon 1a did not have any methionines that are in-frame with the nesprin-3α Y2H polypeptide (Fig. S1 A). Although exon 1a was the most frequently detected first exon in both cell lines, we did identify multiple other exon 1 splice variants of nesprin-3 (exons 1c, 1c′, 1d, 1e, and 1f; Fig. S1 B). Three of the alternative exon 1 sequences, exons 1c′, 1d, and 1e, contain upstream in-frame stop codons that preclude the possibility of any additional start sites for translation, but two exon 1 sequences, exons 1c and 1f, contain other potential start sites of translation that would encode for an additional 38 and 30 amino acids upstream of the initiation methionine of nesprin-3α, respectively (Fig. S1 B). Longer nesprin-3 variants in the nesprin-3β reading frame are not

possible because of a stop codon in exon 2 just upstream of the starting methionine (Fig. S1 A). The results of the 5′-RACE analysis suggest that transcript variants equivalent to the long isoforms of nesprin-1 and -2 do not exist of nesprin-3.

Distribution of nesprin-3 in cell lines and tissues

To further characterize the nesprin-3 protein, rabbit polyclonal antibodies (pAbs) were generated against the seventh SR of murine nesprin-3 and, subsequently, the pAbs were tested for their specificity to nesprin-3 (Fig. S2, available at http://www.jcb.org/cgi/content/full/jcb.200506083/DC1). We first tested the expression of nesprin-3 in 14 different mouse-derived cell lines. A band of ~110 kD, corresponding to nesprin-3α, was detected in all 14 cell lines tested, suggesting that this variant of nesprin-3 is ubiquitously expressed (Fig. 3 A). We did not detect any higher molecular mass bands in any of these cell lines, which is consistent with the notion that we are dealing with the full-length nesprin-3 protein.

We next tested the expression of nesprin-3 in several different mouse tissues and in all of these tissues we detected the 110-kD protein (Fig. 3 B). A 97-kD protein reacting with the nesprin-3 antibody is likely a degradation product of the nesprin-3α protein because this band is also present in the lysates of the vesicular stomatitis virus (VSV)-nesprin-3α–transfected COS7 cells. These results indicate that nesprin-3 is ubiquitously expressed in tissues and most likely represents the largest and most widely expressed splice variant of nesprin-3.

To verify this at the mRNA level, we used an RT-PCR–based method to detect the presence of either nesprin-3α or -3β in three different cell lines. We used primers that anneal in exon 2 and 4, thus encompassing the nesprin-3α–specific exon 3. A PCR band of 228 bp represents nesprin-3β and a band of 401 bp represents nesprin-3α because of the inclusion of the 173 bp of exon 3. We also performed a control RT-PCR reaction that would amplify a region of nesprin-3 from exon 15–18, which includes the KASH domain–encoding sequence (Fig. 3 C). For both primer pairs, PCRs of the nesprin-3α and -3β cDNA–containing plasmids were included as controls (Fig. 3 C). The results showed that in three different mouse-derived cell lines, NMK-1, mTSC, and mBCC-1, the predominant nesprin-3 splice variant was 3α, although its expression level differed (Fig. 3 C). This is consistent with the results obtained from the Western blots of the same mouse cell lines (Fig. 3 A).

Nesprin-3 is localized at the ONM

To determine the subcellular location of nesprin-3, we transiently transfected pyloric atresia associated with junctional epidermolysis bullosa (PA-JEB) keratinocytes with constructs expressing GFP- or VSV-tagged nesprin-3α and -3β proteins. The results indicate that GFP-nesprin-3α and -3β are localized at the NE, although there is some staining within the nucleus, which is likely caused by the folding of the NE. The location of nesprin-3 was confirmed by colocalization studies with endogenous lamin A, which is a structural protein known to reside at the nucleoplasmic side of the INM (Fig. 4 A). Immunofluorescence studies of the VSV-tagged nesprin-3α and -3β proteins

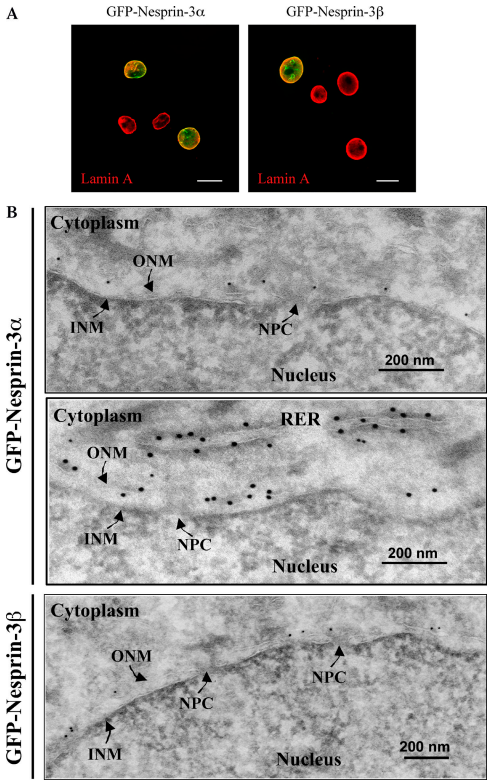

Figure 4. **Subcellular localization of nesprin-3α and -3β.** (A) To determine the subcellular location of nesprin-3, PA-JEB keratinocytes were transiently transfected with either GFP-nesprin-3α or -3β cDNA, and the expression pattern was analyzed by fluorescence microscopy. Immunofluorescence studies of endogenous lamin A were performed using mAb 133A2. Bar, 20 μM. Four cells are shown in each image. (B) To determine which lipid bilayer of the NE contains nesprin-3, ultrathin sections of PA-JEB cells stably expressing either nesprin-3α (top and middle) or -3β (bottom) were labeled with rabbit pAbs against GFP, followed by incubation with 15-nm gold-conjugated protein A. NPC, nuclear pore complex.

and endogenous nesprin-3 also showed localization at the NE and, in some cells, at the RER (Fig. 5 B and not depicted). Together, these results definitively show that nesprin-3 is a NE component. The results also indicate that the GFP and VSV tags do not affect the localization of the nesprin-3 proteins. Because confocal microscopy is not sensitive enough to determine which lipid bilayer of the NE contains nesprin-3, we used EM analysis on PA-JEB cells stably expressing either GFP-nesprin-3α or -3β. Using antibodies directed against the GFP moiety, we were able to show that, like nesprin-1 and -2, nesprin-3 is also present in the ONM (Fig. 4 B; Starr and Han, 2002; Zhen et al., 2002). Furthermore, some cells showed strong staining of nesprin-3 in the RER (Fig. 4 B), which was always correlated with a higher level of nesprin-3 expression in individual cells (Fig. 5 B).

Nesprin-3α is associated with plectin at the ONM

To verify the results of the Y2H assay, we coexpressed cDNAs of VSV-nesprin-3α and -3β, along with cDNAs encoding either a HA-tagged plectin-1A or -1C ABD, a HA-tagged MACF ABD, which has an ABD similar to that of plectin

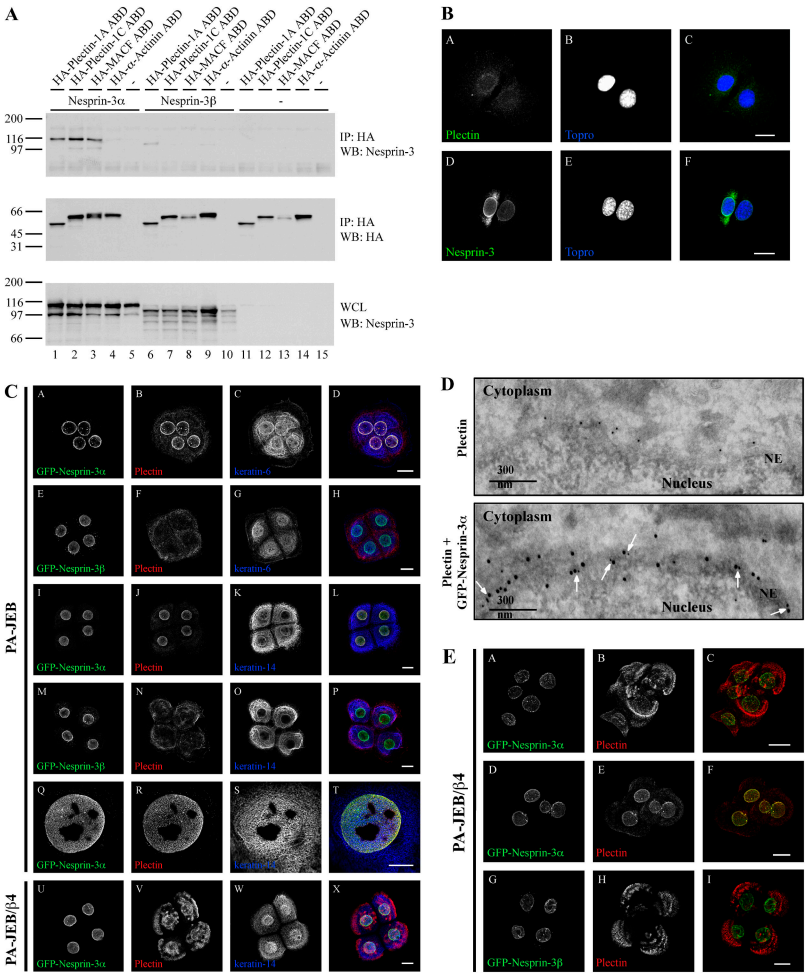

Figure 5. **Nesprin-3α associates with plectin in cells.** (A) COS7 cells were transiently transfected with either the nesprin-3α (lanes 1–5) or -3β (lanes 6–10) cDNA constructs, or a control plasmid (lanes 10–15) and expression constructs for the HA-plectin-1A ABD (lanes 1, 6, and 11), HA-plectin-1C ABD (lanes 2, 7, and 12), HA-MACF ABD (lanes 3, 8, and 13), HA-α-actinin-1 ABD (lanes 4, 9, and 14), or a control plasmid (lanes 5, 10, and 15). The cells were lysed in RIPA buffer and HA-IPs were probed for the presence of nesprin-3 (top) and the HA-tagged ABDs (middle). WCLs were probed for expression levels of the two different nesprin-3 isoforms (bottom). (B) MEF cells were stained for endogenous plectin using the mAb 121 (A) and nesprin-3 using rabbit pAbs (D). The location of the nucleus was visualized using Topro staining (B and E). C is a composite of A and B, and F is a composite of D and E. Bar, 20 μM. (C) PA-JEB (A–T) or PA-JEB/β4 (U–X) were stably transduced with retroviral constructs expressing either GFP-nesprin-3α (A–D, I–L, and Q–X) or GFP-nesprin-3β (E–H and M–P). Fluorescence studies were done to locate the GFP moiety (A, E, I, M, Q, and U), along with immunofluorescence studies of endogenous plectin (B, F, J, N, R, and V) and keratin-6 (C and G) or keratin-14 (K, O, S, and W). The far right image of each row depicts the composite image of the first three images in each row (D, H, L, P, T, and X). Four cells are shown in each image except for images Q–T, which show a higher magnification of the nucleus. All images are maximum projections. Bars: (A–P and U–X) 20 μM; (Q–T) 10 μM. (D) To determine the subcellular localization of nesprin-3 and plectin at the NE, ultrathin sections of PA-JEB cells stably expressing nesprin-3α were labeled with rabbit pAbs against the plectin-ABD (D16), followed by incubation with 10-nm gold-conjugated protein A. The sections were then fixed in 1% glutaraldehyde and reprobed with rabbit pAbs against GFP, followed by incubation with 15-nm gold-conjugated protein A. Arrows indicate areas where plectin and GFP-nesprin-3α are colocalized at the ONM (bottom). Control labeling was done in the same way, except that after plectin labeling and fixation in glutaraldehyde, the sections were reprobed with 15-nm gold-conjugated protein A only (top). Note that no labeling with 15-nm gold was seen at the NE. (E) PA-JEB/β4 cells stably expressing either GFP-nesprin-3α (A–F) or GFP-nesprin-3β (G–I) were visualized for GFP (A, D, and G) and plectin (B, E, and H). The far right image of each row depicts the composite image of the first two images in each row (C, F, and I). All images are maximum projections. Bar, 20 μM.

(76% homology), or a HA-tagged α-actinin-1 ABD in COS7 cells. To test the ability of the nesprin-3 proteins to bind to the different ABDs, immunoprecipitations were prepared with anti-HA antibodies and tested for the presence of the different nesprin-3 splice variants. Consistent with the findings shown in Fig. 1, the results of the pull-down assay show that nesprin-3α strongly interacts with the ABDs of plectin-1A and -1C, but not with that of α-actinin-1. Interestingly, nesprin-3α can also interact with the MACF ABD (Fig. 5 A). Unexpectedly, nesprin-3β only weakly interacted with any of the ABDs tested. This result suggests that the first SR is critical for the high affinity binding of nesprin-3α to the plectin and MACF ABDs and we have therefore named this region of nesprin-3α the plakin-binding domain. These results were later confirmed by using a cDNA of nesprin-3α of which the upstream, noncoding sequences that were present in the original Y2H clone had been removed, verifying the importance of the SR1 in mediating binding to the plectin and MACF ABDs (Fig. S1 A and not depicted).

The results thus far indicate that nesprin-3α can directly associate with plectin at the ONM. To verify these results, we used immunofluorescence studies on these proteins in cells. We first looked at the location of endogenous nesprin-3 and plectin in mouse embryonic fibroblast (MEF) cells. The results show that nesprin-3 is indeed present at the NE, but that plectin is not obviously concentrated at the nuclear perimeter, although it is present throughout the cytoplasm (Fig. 5 B). One possible reason for the relatively low concentration of plectin at the NE may be the ability of the actin cytoskeleton to bind and sequester plectin (Wiche, 1998), thereby limiting the amount of plectin available for interacting with nesprin-3α. To test this notion, we stably overexpressed GFP-nesprin-3α or -3β into PA-JEB or PA-JEB/β4 cells and performed colocalization studies with plectin. We hypothesized that nesprin-3α, but not nesprin-3β, when overexpressed, competes with actin for binding to plectin, resulting in the sequestration of plectin at the NE. To determine whether plectin, when bound to nesprin-3α, can also associate with IFs, we also labeled cells with antibodies that recognize keratin-6 and -14. The results show that nesprin-3α can strongly recruit plectin to the ONM in both the PA-JEB and PA-JEB/β4 cells and, consistent with the findings shown in Fig. 5 A, nesprin-3β did not recruit plectin to the NE. The keratin-6 and -14 IF proteins are also strongly stained at the nuclear perimeter, which infers that plectin may mediate the association of the IFs to nesprin-3α at the NE (Fig. 5 C).

In addition, a higher magnification of the nucleus showed almost equally strong staining of nesprin-3α, plectin, and keratin-6 at the ONM (Fig. 5 C). We also performed EM studies to determine the exact location of plectin and GFP-nesprin-3α in PA-JEB cells. The results confirm that nesprin-3α and plectin are situated together at the ONM (Fig. 5 D). These findings clearly demonstrate that nesprin-3α can bind plectin at the ONM in cells. Intriguingly, the results also suggest that plectin may mediate the linkage of nesprin-3α with the keratin-6/16 and -5/14 IF systems.

We also decided to make use of a GFP-nesprin-3α construct, which lacks the KASH domain but contains the sequence present in the original Y2H clone (GFP-nesprin-3α$^{\Delta KASH}$; Fig. 2 C). This clone retains the sequences necessary to bind plectin, but because of the absence of the KASH domain it is not localized at the ONM and instead displays a filamentous cytoplasmic and nuclear distribution (Fig. S3, available at http://www.jcb.org/cgi/content/full/jcb.200506083/DC1). We stained for plectin along with either keratin-5 or F-actin in PA-JEB cells transiently expressing GFP-nesprin-3α$^{\Delta KASH}$ to determine whether it had any effect on the distribution of these proteins. GFP-nesprin-3α$^{\Delta KASH}$ did not significantly alter the distribution of plectin and was only partially colocalized with plectin in the cytoplasm of the PA-JEB cells (Fig. S3). However, the GFP-nesprin-3α$^{\Delta KASH}$ proteins were specifically localized along the keratin-5 IFs and they did not become localized with the actin cytoskeleton (Fig. S3). Because nesprin-3α binds to the ABD of plectin, the plakin repeats are free to make associations with the IF cytoskeleton, which can partially account for the localization of GFP-nesprin-3α$^{\Delta KASH}$ along IFs and, similarly, GFP-nesprin-3α$^{\Delta KASH}$ will compete with actin for binding to the plectin ABD, which is why it was not present along actin filaments. The observed imaging of GFP-nesprin-3α$^{\Delta KASH}$ along IFs in the absence of plectin staining may be a result of other plectin isoforms that are present in PA-JEB cells that are not recognized by the mAb 121 against plectin (i.e., the rod-less variant; Fig. S3). Additionally, the filamentous patterning of GFP-nesprin-3α$^{\Delta KASH}$ in the absence of keratin-5 staining is most likely caused by the association of these proteins with other IF networks (Fig. S3). Together, the nesprin-3α proteins lacking the KASH domain do not obviously affect the IF network or the distribution of plectin, but they do provide additional evidence that plectin links nesprin-3α to the IF cytoskeleton.

The integrin α6β4 and nesprin-3α both associate with plectin in keratinocytes

Our findings suggest the possibility that in basal keratinocytes plectin links the IFs to nesprin-3α at the ONM and to integrin α6β4 at hemidesmosomes at the plasma membrane. This would allow for a continuous protein scaffolding from the extracellular environment to the nucleus. We decided to take a closer look at PA-JEB/β4 cells that stably express either GFP-nesprin-3α or GFP-nesprin-3β. In most PA-JEB/β4 cells expressing GFP-nesprin-3α, we saw staining of plectin at the NE and the presence of plectin in hemidesmosomes (Fig. 5 C). However, in some PA-JEB/β4 cells expressing GFP-nesprin-3α, there was almost no staining of plectin at the NE, which coincided with a strong expression of plectin in hemidesmosomes, or alternatively, in some cells there was strong staining of plectin at the NE with almost no hemidesmosomal staining (Fig. 5 E). This effect was never seen in PA-JEB/β4 cells expressing GFP-nesprin-3β, which consistently showed hemidesmosomal staining of plectin (Fig. 5 E). These results suggest that β4 and nesprin-3α compete for binding to the same pool of plectin and, moreover, that plectin may link these two proteins to the same IF cytoskeleton.

Endogenous nesprin-3 and plectin associate in cells

To verify that endogenous nesprin-3α and plectin can associate at the ONM in cells, we used small interfering RNA (siRNA) knock-down of nesprin-3 in the mouse Sertoli cell line TM-4. We selected these cells because it has previously been reported that there is a high concentration of plectin around their nuclear perimeter (Guttman et al., 1999), and therefore any effects on plectin redistribution will be more easily detected. As expected, nesprin-3 is expressed in TM-4 cells (Fig. S4 A, available at http://www.jcb.org/cgi/content/full/jcb.200506083/DC1). We then designed a siRNA construct in a region of the mouse nesprin-3 cDNA that was present in both splice variants and tested its efficacy by coexpressing cDNAs of VSV-nesprin-3α and -3β, along with cDNAs encoding either the nesprin-3 siRNA, a luciferase control siRNA, or an empty vector control plasmid in human-derived 293 human embryonic kidney cells. The results show that the nesprin-3 siRNA specifically knocks down the expression of transiently expressed nesprin-3α and -3β proteins (Fig. S4 B).

We next wanted to verify that the nesprin-3 siRNA can knock-down the expression of the protein in TM-4 cells and to determine the location of plectin in these cells. The nesprin-3 siRNA– or luciferase control siRNA–containing vectors were independently transfected into TM-4 cells, along with a monomeric red fluorescent protein (mRFP) expression plasmid, and the cells were stained for endogenous plectin and nesprin-3 (Fig. 6 A). The mRFP protein was visualized to determine whether the cells express the siRNAs. The results show that the nesprin-3 siRNA can specifically knock-down the expression of the protein at the NE in TM-4 cells. The results also show that the knock-down of nesprin-3 does not obviously affect the distribution of plectin, but do show that in some cells plectin is concentrated around the NE as reported previously (Guttman et al., 1999). Interestingly, in fully spread cells plectin is primarily present in FCs and colocalized with F-actin (Fig. 6 B). Like that from MEF cells, the data obtained from TM-4 cells suggests that nesprin-3α and actin filaments compete for binding to plectin. Therefore, we decided to disrupt the actin network in TM-4 cells using latrunculin B. This should have resulted in an increased amount of plectin available to interact with nesprin-3α at the ONM and, indeed, this is what was observed (Fig. 6 B). To determine if the recruitment of plectin to the nuclear perimeter is dependent on the presence of nesprin-3α, we expressed the nesprin-3 siRNA–containing vector in TM-4 cells and treated the cells with latrunculin B. The concentration of plectin around the nuclear perimeter in these cells was significantly

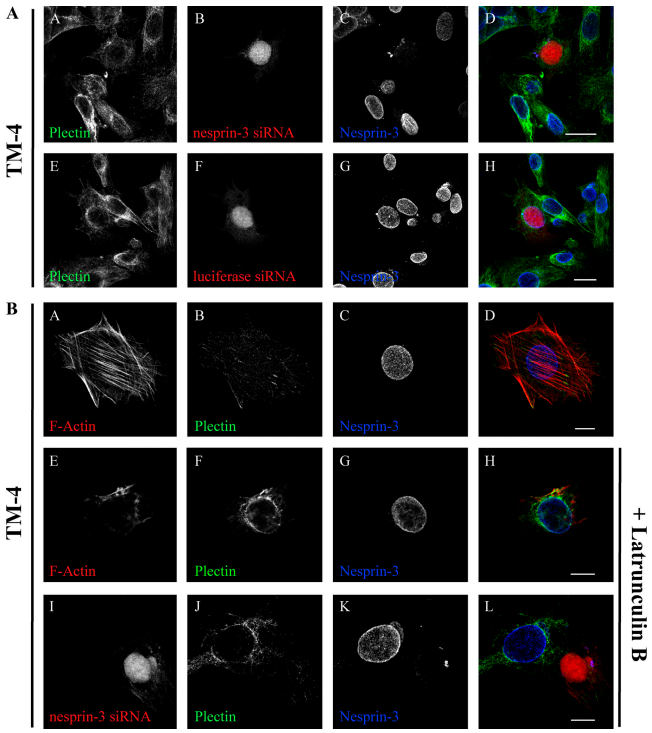

Figure 6. **Endogenous nesprin-3 and plectin associate in TM-4 cells.** (A) The mouse Sertoli cell line TM-4 was transiently transfected with either the pSUPER vector expressing the nesprin-3 siRNA (A–D) or the luciferase siRNA (E–H), along with an expression vector for mRFP at a 5:1 ratio. After 72 h, the cells were fixed and stained for endogenous plectin (A and E) and nesprin-3 using our pAbs (C and G). mRFP was visualized to determine which cells express the siRNAs (B and F). D and H are composite images of the first three images in each row. All images are maximum projections. Bar, 20 μM. (B) TM-4 cells were left untransfected (A–H) or transiently transfected with the pSUPER vector expressing the nesprin-3 siRNA, along with an expression vector for mRFP in a 5:1 ratio (I–L). After 72 h and just before fixation, the cells in images E–L were treated for 30 min with 0.2 μM latrunculin B. The cells were then fixed and stained for plectin (B, F, and J), nesprin-3 (C, G, and K), and F-actin (A and E). mRFP was visualized to determine which cells express the nesprin-3 siRNA (I). D, H, and L are composite images of the first three images in each row. Bar, 10 μM.

reduced, with plectin now being distributed in the cytoplasm (Fig. 6 B), which suggests that the recruitment of plectin to the ONM after actin depolymerization is indeed dependent on nesprin-3α. These data also infer that the plectin that is concentrated around the nuclear perimeter in cells that were not fully spread is also dependent on an association with nesprin-3α. Together, the data presented thus far clearly demonstrate that nesprin-3α can bind plectin at the ONM in cells.

Nesprin-3α does not associate with MACF at the ONM

The results shown in Fig. 5 A infer that nesprin-3α may also bind MACF at the ONM, which intriguingly suggests that nesprin-3α may connect the nucleus to MTs (Jefferson et al., 2004). We again used the PA-JEB cells, which stably overexpress the GFP-nesprin-3α or -3β proteins, but instead stained them for the presence of endogenous MACF and MTs. The results show that nesprin-3α cannot recruit MACF to the nuclear perimeter even though MTs were present at the NE (Fig. S5 A, available at http://www.jcb.org/cgi/content/full/jcb.200506083/DC1), suggesting that MACF and nesprin-3α do not associate in cells. It is possible, however, that the strong association between plectin and GFP-nesprin-3α in the PA-JEB cells may prevent binding of MACF to nesprin-3α and, thus, its recruitment to the ONM. To investigate this possibility, we stably expressed either the GFP-nesprin-3α or -3β proteins in epidermolysis bullosa simplex with muscular dystrophy (EBS-MD) keratinocytes (Geerts et al., 1999), whose cells do not express full-length plectin and express the rodless variant of plectin at relatively low levels (Koster et al., 2004b). Therefore, if there is competition between plectin and MACF for binding to nesprin-3α, it will be minimal and the recruitment of MACF to nesprin-3α at the ONM should therefore be increased. The results from the immunofluoresence experiments show that there is an increase of MACF staining around the nuclear perimeter as compared with that in the PA-JEB cells. However, this does not appear to depend on the expression of nesprin-3α (Fig. S5 B). Together, these data suggest that, unlike plectin, MACF does not bind to nesprin-3α in cells and that the interaction between plectin and nesprin-3α at the ONM is specific.

Discussion

We have identified nesprin-3 as a novel member of the nesprin family of ONM proteins. One splice variant, nesprin-3α, is able to bind to the plakin family member plectin at the NE. In keratinocytes, nesprin-3α and the integrin β4 subunit both bind to plectin, which also binds to the keratin IF system, suggesting that hemidesmosomes at the cell surface may be connected directly to the nucleus via the same cytoskeletal systems. In contrast, nesprin-3α cannot associate with endogenous MACF in cells, even though the MACF ABD binds to nesprin-3α in coimmunoprecipitation experiments, suggesting that, in cells, the interaction between the plectin ABD and nesprin-3α is specific. We have also identified a minor splice variant, nesprin-3β, which is unable to bind or recruit plectin to the ONM.

Nesprin-1 and -2 are gigantic molecules of ∼976 and 764 kD, respectively. However, several smaller variants of nesprin-1 and -2, which are produced by alternative RNA splicing and/or initiation sites of transcription, have been identified that lack the NH_2-terminal ABD. The structure of nesprin-3 closely resembles that of nesprin-1α and -2β, which suggested to us that nesprin-3α and -3β are most likely smaller splice variants of a larger nesprin-3 molecule. However, several lines of evidence show that this is not the case. First, we could not identify cDNAs in either the mouse or the human databases containing sequences in exons upstream of the alternatively spliced exon 1, and careful analysis of upstream genomic sequences failed to identify sequences present in a calponin homology motif. Second, 5′-RACE-PCR on mRNA from different cell lines failed to identify any longer transcripts containing exons upstream of those for nesprin-3α, as indicated in Fig. 1. Finally, our nesprin-3 pAbs failed to detect any larger nesprin-3 variants in any of the cell lines or tissues we tested. Based on these data, it appears that nesprin-3α is the largest variant of this new nesprin family member.

The results from our immunofluorescence studies using either full-length nesprin-3α or a nesprin-3α protein lacking the KASH domain provide strong, although circumstantial, evidence that plectin can mediate the linkage of the IF cytoskeleton to nesprin-3α at the ONM. This is especially relevant because the IF interaction site and the ABD are on opposite ends of the plectin molecule (~500 kD), therefore it seems unlikely that the binding of plectin to the IF cytoskeleton would interfere with its binding to nesprin-3α. Thus, it is reasonable to conclude that nesprin-3α can indeed link the nucleus to the IF cytoskeleton through plectin. In nesprin-1/2, the KASH domain is located at the COOH-terminus, whereas the ABD is located at the NH_2-terminus at a distance of ~150–200 nm (Starr and Han, 2003). This suggests that there must be a relatively large space between the ONM and the actin cytoskeleton. It became apparent to us that a similar space may be important between the ONM and the IFs because, like nesprin-1/2, plectin is extremely large and when it is bound to nesprin-3α, a comparable distance is achieved. At present, it is not clear why such a space is required between the ONM and the different cytoskeletal systems. It has also been reported that some isoforms of nesprin-1/2 are localized at the INM (Zhang et al., 2001; Libotte et al., 2005). However, we found no concrete evidence that nesprin-3 is so localized. It therefore appears that the nesprin family of proteins have evolved to link the nucleus to the various cytoskeletal systems, either directly (i.e., nesprin-1/2) or indirectly via members of the plakin family (i.e., nesprin-3). However, we detected only subtle, inconsistent effects on the IF cytoskeleton when nesprin-3α was overexpressed or when nesprin-3 was knocked-down by siRNAs. Moreover, our data with the TM-4 cells suggests that plectin may only be associated with nesprin-3α at the ONM during specific cellular events because we consistently saw that plectin was more concentrated around the nucleus when the TM-4 cells were more contracted or when the actin cytoskeleton was disrupted, whereas there is very little plectin around the nucleus in fully spread cells containing well defined actin stress fibers. It is possible that the function of nesprin-3α is to sequester plectin during such processes as cell division or migration when the cells contract and become more rounded because of cytoskeletal rearrangements.

We have also identified a splice variant of nesprin-3 that is unable to associate with plectin. The original nesprin-3β RIKEN clone 4831426I19 is derived from head tissue of a day 0 neonatal mouse. Consistent with the origin of the RIKEN clone, we observed a faint protein band corresponding to the molecular mass of nesprin-3β in a lysate derived from brain tissue. However, nesprin-3β is not ubiquitously or strongly expressed in cells because we did not detect it by Western blotting or RT-PCR analysis in several different cell lines and tissues. The existence of this splice variant suggests that nesprin-3 must have functions other than connecting the nucleus to the IFs or sequestering plectin.

The results of our Y2H and pull-down assays show that nesprin-3α and the β4 subunit have the same binding specificity for the different ABDs. We found this surprising because the plectin ABD binding region on the first pair of FNIII domains of β4 (i.e., β sheets; de Pereda et al., 1999) is structurally very

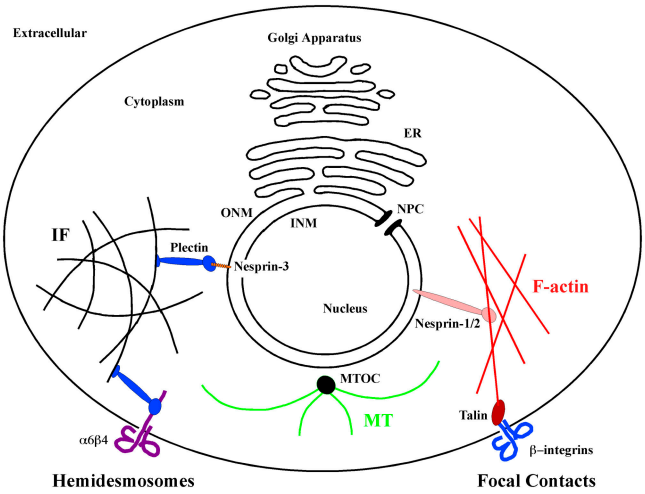

Figure 7. **Model depicting how the nesprins can link the nucleus to the actin and IF cytoskeletal systems.** Nesprin-3 at the ONM and the integrin β4 subunit at the cell surface are shown bound to the NH_2-terminal plectin ABD. COOH-terminal plectin plakin repeats are free to make associations with IFs, thus linking the nucleus to the hemidesmosomes at the cell surface. In an analogous way, nesprin-1/2 and talin, bound to the cytoplasmic tail of β integrins, interact with the actin filaments, which link the nucleus to FCs (black, IF cytoskeleton; green, MT system; red, F-actin). MTOC, MT organizing center.

different from the SRs in nesprin-3α (i.e., α-helices; Yan et al., 1993). In fact, our original Y2H screen with the plectin-1C ABD also identified a novel interaction with an SR-rich region of β2-spectrin, suggesting that the binding of an ABD to SRs is not unique for nesprin-3 (unpublished data). It has been shown previously that the binding of the plectin ABD to the β4 FNIII domains and to actin is mutually exclusive (Geerts et al., 1999). Because of the similarities in binding specificity, we believe that this is also true for the binding of the plectin ABD to nesprin-3α and actin, although competition studies will have to prove this. If confirmed, this would suggest that in a cell the recruitment of plectin to actin filaments and to nesprin-3α is competitive, which could partially explain why we saw minimal staining of plectin at the nuclear perimeter in cells with well-defined actin stress fibers, but saw recruitment of plectin to the ONM when nesprin-3α was overexpressed or when the actin cytoskeleton was disrupted. Our results also show that nesprin-3α can bind the ABDs of MACF and BPAG1-n. These two proteins would allow nesprin-3α to also link the nucleus to MTs. However, we could not confirm an interaction between full-length MACF and nesprin-3α in PA-JEB or EBS-MD keratinocytes, suggesting that the endogenous proteins do not associate or that the binding between the MACF ABD and nesprin-3α is regulated differently in these cells.

Our finding that in keratinocytes nesprin-3α can compete with the integrin β4 subunit for binding to plectin suggests that these two molecules are connected to the same IF system. Indeed, immunofluorescence studies showed that the keratin-14 IF system is colocalized with both plectin at the NE and plectin in hemidesmosomes (Geerts et al., 1999). This implies that plectin can be the link in a continuous protein scaffold from the extracellular matrix to the nucleus via the IF cytoskeleton (Fig. 7),

analogous to the manner in which nesprin-1/2 can link the nucleus to FCs at the plasma membrane via actin filaments (Fig. 7). This notion is consistent with the cellular tensegrity model, which describes the cell as a prestressed structure whereby forces can be transferred from the extracellular environment through the different cytoskeletons into the nucleus (Ingber, 2003a,b). This model integrates and explains many observations in cell biology, such as nuclear architecture, but importantly it can explain how external forces may affect events in the nucleus such as chromatin organization (Maniotis et al., 1997). The nesprins are the prime candidates for mediating these processes because they have been shown to interact with INM proteins associated with the nuclear lamins (Gruenbaum et al., 2005). The lamins are known to bind chromatin and have even been suggested to play a role in regulating transcription by RNA polymerase II and DNA replication (Spann et al., 1997, 2002). If force can indeed directly alter gene expression, the need for cytoplasmic signaling events would be circumvented, allowing for a more instantaneous regulation of transcriptional events during cell migration or situations of applied force. Although these ideas are intriguing, clearly more studies are necessary to determine the extent to which the nesprins can mediate the transfer of force into the nucleus.

Materials and methods

Y2H assay

A Y2H screen with a mouse embryonic day 17 cDNA library (CLONTECH Laboratories, Inc.) cloned into the yeast *Gal4* transcriptional activation domain (AD) expression vector pGAD10 (CLONTECH Laboratories, Inc.) was performed. The cDNA sequence of the human plectin-1C ABD, which was fused in-frame to the *Gal4* DNA-binding domain (BD) of the pAS2.1 vector (CLONTECH Laboratories, Inc.), was used as bait (Geerts et al., 1999). Plasmids were introduced into the yeast strain PJ69-4A (a gift from P. James, University of Wisconsin, Madison, WI) by transformation, as described in the CLONTECH two-hybrid manual. Protein–protein interactions between bait and prey were confirmed by cotransformation into PJ69-4A, as described previously (Schaapveld et al., 1998; Geerts et al., 1999). Expression of the fusion proteins in yeast was confirmed by immunoblotting with *Gal4*(BD)- and *Gal4*(AD)-specific antibodies (Santa Cruz Biotechnology, Inc.).

Cell lines, antibodies, and other reagents

COS7 and MEF cells were grown in DME (Life Technologies) containing 10% fetal calf serum, 100 U/ml penicillin, and 100 U/ml streptomycin. COS7 cells were transiently transfected with cDNA constructs using the DEAE-dextran method (Seed and Aruffo, 1987), and MEF cells were transfected with Effectene (QIAGEN). The PA-JEB and EBS-MD keratinocyte cell lines were maintained in keratinocyte serum-free medium (Life Technologies) supplemented with 50 μg/ml bovine pituitary extract, 5 ng/ml EGF, 100 U/ml penicillin, and 100 U/ml streptomycin. The mouse Sertoli cell line TM-4 was maintained in DME containing 2.5% fetal calf serum, 5% horse serum, 15 mM Hepes, pH 7.4, 100 U/ml penicillin, and 100 U/ml streptomycin. The following mouse-derived cell lines were also used: Tam2D2-lymphoma; N115-neuroblastoma; GE11-epithelial; C2C12-myoblast; J774-macrophage; NMK-1-keratinocyte; mTSC-tumor stem cell; mBCC-1-basal cell carcinoma; and RAC-11P and mSCC-1, -2, -3, -4-squamous cell carcinoma. Stable integration of the β4 integrin and GFP-nesprin-3α/β were performed as described previously (Sterk et al., 2000). Murine nesprin-3 rabbit pAbs were raised against the seventh SR (Fig. S1 A) common to both 3α and 3β and fused to GST (see cDNA constructs for specifics). This antigen sequence shows 93% (rat), 67% (dog), 64% (human), 63% (chimpanzee), and 43% (chicken) homology to the same region of nesprin-3 in other species. This sequence also shows 34% homology to nesprin-1 (mouse) and 23% homology to spectrin-β2 (mouse), and is therefore not likely to cross react. The lamin A mAb (133A2) was a gift from F. Ramaekers (University of Maastricht, Maastricht, Netherlands). The mouse mAb 121 against plectin/HD1 was provided by K. Owaribe (University of Nagoya, Nagoya, Japan; Hieda et al., 1992). The monoclonal β4 antibody (450-11A) was purchased from BD Biosciences. The monoclonal tubulin antibody was obtained from Sigma-Aldrich. The polyclonal MACF antibody CU119 was a gift from R. Liem (Columbia University, New York, NY) and has been described previously (Lin et al., 2005). The polyclonal GFP antibody was made at Sanquin Blood Supply Foundation and has been described previously (van Ham et al., 1997). The affinity column–purified plectin ABD rabbit pAb (D16) was made as described previously (Geerts et al., 1999). Keratin-5, -6 (PRB-169P), and -14 (AF64) rabbit pAbs were purchased from Covance Research Products, Inc. The HA mAb (12CA5) and polyclonal HA antibody (Y-11) were purchased from Santa Cruz Biotechnology, Inc.; the donkey anti–rabbit and goat anti–mouse horseradish peroxidase–conjugated antibodies were purchased from GE Healthcare; the goat anti–mouse FITC-conjugated antiserum was obtained from Rockland Immunochemicals, Inc.; and the goat anti–rabbit Texas red–conjugated antibodies were purchased from Invitrogen. Phalloidin-Texas red and latrunculin B were purchased from Sigma-Aldrich and TOP-RO was obtained from Invitrogen.

cDNA constructs

pcDNA3-VSV was generated by inserting a 100-bp fragment, containing two VSV tags (YTDIEMNRLGK) flanked by KpnI, ClaI, and NcoI sites upstream and a BamHI site downstream, into the KpnI–BamHI sites of pcDNA3 (Invitrogen).

Nesprin-3. PCR fragments of nesprin-3β (clone 4831426I19; RIKEN) were cloned into the BamHI–EcoRV sites of the pcDNA3-VSV vector in two steps. First, the COOH-terminal part containing the sequence starting from the internal BamHI site (exon 10) until the end was cloned, and, second, the NH_2-terminal part until the internal BamHI site was inserted. The published sequence for the clone contains a single cytosine nucleotide insertion just after position 2,652. The original nesprin-3α construct was made by inserting the NH_2-terminal fragment (containing the upstream, noncoding sequences present in the Y2H clone [Fig. S1 A]) until the internal BamHI site into a pcDNA3-VSV vector that already contained the COOH-terminal part of nesprin-3β. A nesprin-3α construct was also made that had the upstream, noncoding sequences removed. This was done by inserting a PCR fragment that was generated from a primer annealing to the internal BamHI site and a primer containing an upstream BamHI site fused to sequences annealing to nucleotides that encode for the first six amino acids of nesprin-3α (Fig. S1 A) into the original nesprin-3α pcDNA3-VSV vector using BamHI–BamHI sites. Nesprin-3α was cloned into pEGFP-C3 (CLONTECH Laboratories, Inc.) using HindIII–EcoRI sites. Subsequently, nesprin-3α in pLZRS-IRES-zeo was obtained by first inserting GFP into the BamHI–EcoRI sites of this vector with subsequent insertion of the EcoRI digest of nesprin-3α from pEGFP-C3. Nesprin-3β was cloned into pEGFP-C3 using HindIII–SalI sites. The NheI–SalI sites of this construct were used to obtain the GFP-nesprin-3β fragment for cloning into the SwaI–XhoI sites of pLZRS-IRES-zeo. The NheI site was blunt ended using T4 polymerase. The nesprin-3α lacking the KASH domain (GFP-nesprin-$3\alpha^{\Delta KASH}$) construct was made by amplifying the region of the nesprin-3α sequence identified in the original Y2H plasmid (Fig. S1 A) with primers containing BamHI and XbaI restriction sites, and this PCR fragment was then subsequently cloned into the pcDNA3-VSV vector. The insert was then cut out of pcDNA3-VSV with HindIII and XbaI and the XbaI site was then blunt ended. The pEGFP-C3 vector (CLONTECH Laboratories, Inc.) was cut with HindIII and EcoRI and the EcoRI site was blunt ended. The insert was then cloned into this vector.

HA-tagged ABDs. The HA-tagged plectin constructs have been described previously (Litjens et al., 2003). The sequence for the BPAG1-n (dystonin-1) ABD (amino acids 1–388) in pcDNA3-HA was generated by PCR using BamHI–NotI restriction sites. The MACF ABD cDNA sequence (amino acids 1–327) in pcDNA3-HA was generated by digestion out of a construct provided by R. Liem using EcoRI–BamHI restriction sites. The α-actinin-1 ABD cDNA (amino acids 1–337) in pcDNA3-HA was generated by PCR using EcoRI–NotI restriction sites. Both the α-actinin-1 and BPAG1-n ABD cDNAs in pAS2-1 on which the PCRs were performed have been described previously (Litjens et al., 2003). The GST-nesprin-3-SR7 antigen was made by cloning the nesprin-3 SR7–derived PCR product (using primers 5′-cgcggggaattcccaccttcagtcacaggctg-3′ and 5′-ggccgcgcggccgctctcatgagactcagcat-3′) into pGEX-4T-2 (GE Healthcare) digested with EcoRI and NotI. GST preparations were done as previously described (Wilhelmsen et al., 2002) and fusion proteins were eluted from glutathione-Sepharose beads using 15 mM of reduced glutathione. All PCR fragments were generated using the proofreading *Pwo* DNA polymerase (Roche). All plasmids were verified by sequencing, and protein expression and size were confirmed by Western blotting.

Coimmunoprecipitation experiments

Cells were grown to confluency on 10-cm tissue culture dishes, rinsed twice with cold TBS, and lysed in 1 ml of 10 mM Na-phosphate, pH 7.0, 150 mM NaCl, 1% NP-40, 1% DOC, 0.1% SDS, 2 mM EDTA, 50 mM NaF, 100 μM sodium vanadate, 10 μg/ml aprotinin, and 10 μg/ml leupeptin (radioimmunoprecipitation [RIPA]-lysis buffer) per 10-cm tissue culture dish. Lysates were cleared by centrifugation at 10,000 rpm in a microfuge at 4°C for 45 min. Nesprin-3 proteins were immunoprecipitated by incubation of cell lysates with 100 μl of a 10% slurry of polyclonal anti–Nesprin-3-SR7 antiserum coupled to protein A–Sepharose beads with dimethyl pimelimidate dihydrochloride (Sigma-Aldrich) with rocking for 1 h at 4°C. Immunoprecipitates were washed four times with 1 ml RIPA-lysis buffer, boiled for 5 min in 62.5 mM Tris/Cl, pH 6.8, 10% glycerol, 5% β-mercaptoethanol, 5 mM DTT, 2.3% SDS, and 0.025% Bromophenol blue (SDS–sample buffer) and resolved by SDS-PAGE. For anti-HA immunoprecipitates, cell lysates were incubated by rocking for 1 h at 4°C with 100 μl of a 10% slurry of anti-HA mAb prebound to γ-bind–Sepharose (GE Healthcare) in the presence of 1% BSA.

Immunofluorescence

PA-JEB, EBS-MD, and MEF cells were grown on glass coverslips, fixed with either 1 or 3% paraformaldehyde in PBS for 10 min, and permeabilized with 0.5% Triton X-100 in PBS for 5 min at room temperature. The TM-4 cells were fixed and permeabilized with 1% paraformaldehyde containing 0.5% Tween 20 in PBS for 10 min. After washing in PBS and blocking with 2% BSA in PBS for 60 min at room temperature, the cells were incubated with primary antibodies for 45 min at room temperature and then washed three times with PBS. Cells were then incubated with either FITC, Cy5, or Texas red–labeled secondary antibodies for 45 min at room temperature. Coverslips were washed three times in PBS, mounted in Mowiol/DAPCO, and viewed under a confocal scanning laser microscope (model SP-2 AOBS; Leica) at room temperature. Images were visualized with either a PL APO 40×, 1.25 NA, or a PL APO (CS) 63× 1.4 NA objective lens (Leica) using LCS software and captured with a photomultiplier.

EM slides

EM was done as previously described (Sterk et al., 2000), with the following modifications. Ultrathin sections of cells were fixed in 2% paraformaldehyde and were either labeled with rabbit pAbs against the plectin-ABD (D16), followed by incubation with 10-nm gold-conjugated protein A, or labeled with rabbit pAbs against GFP, followed by incubation with 15-nm gold-conjugated protein A.

Nesprin-3 siRNA

The mouse nesprin-3 sequence (5′-gctacgtagaatcatcaca-3′) and luciferase sequence used for siRNA knock-down studies was cloned into the pSUPER vector (Brummelkamp et al., 2002). The vectors were transfected into TM-4 cells using the effectene protocol (QIAGEN) and 293 human embryonic kidney cells using the lipofectamine protocol (Invitrogen). The cells were lysed with RIPA buffer or fixed 72 h after transfection and assayed for nesprin-3 expression.

Exon detection primers

In Fig. 3 C, the primers annealing to either side of the nesprin-3α–specific exon 3 were 5′-gagcggccctggaggcaaggcttc-3′ (primer 1) and 5′-caggagcacagcctgattgtccac-3′ (primer 2), and the primers amplifying exons 15–18 of nesprin-3 were 5′-gaacagtggctgcaggcag-3′ (primer 3) and 5′-ggtgggcgggggggccattgtaccg-3′ (primer 4). We also used primers annealing in exon 4 (5′-cgcatcgagtgggtgtggctgcac-3′) and exon 10 (5′-gtccttgtgctgaacaagcaggct-3′) to determine if other potential downstream splice variants exist.

RACE-PCR

5′-RACE-PCR to determine the 5′-sequences of nesprin-3 was performed using the second generation 5′/3′ RACE-PCR (Roche) according to the manufacturer's specifications. Antisense primers annealing to the 5′ end of the known nesprin-3 sequence used in the RACE reactions were 5′-caggagcacagcctgattgtccac-3′, 5′-cacgttgtgcagcagcacctg-3′, and 5′-atcctccacgctcctctc-3′.

Database mining (websites)

Information pertaining to this study is available at the following websites: ELM (www.elm.eu.org), ClustalW (www.ebi.ac.uk/clustalw), SMART (smart.embl-heidelberg.de), basic local alignment search tool (www.ncbi.nih.gov/BLAST), mouse genome research (www.ncbi.nih.gov/genome/guide/mouse), and human genome research (www.ncbi.nlm.nih.gov/genome/guide/human).

Online supplemental material

Fig. S1 A shows the organization of the nesprin-3α cDNA, whereas Fig. S1 B lists all the alternative exon 1 sequences that were detected for nesprin-3 by 5′-RACE-PCR. In Fig. S2, the specificity of the nesprin-3 pAb that was generated against the seventh SR is demonstrated. Fig. S3 is a confocal microscopy image showing that the nesprin-3 proteins lacking the KASH domain are localized along keratin-5 IFs and not along F-actin. Fig. S4 A biochemically confirms that TM-4 cells express nesprin-3 and Fig. S4 B demonstrates the knock-down specificity of the siRNAs that were designed against nesprin-3. Finally, the data in Fig. S5 B indicates that nesprin-3α cannot associate with full-length MACF in keratinocytes. Online supplemental material is available at http://www.jcb.org/cgi/content/full/jcb.200506083/DC1.

We would like to thank Dr. P. James for the yeast strain PJ69-4A and Drs. F. Ramaekers, R. Liem, and K. Owaribe for antibodies.

This work was supported by grants from the Dutch Cancer Society and the Netherlands Science Organization (Netherlands Organisation of Scientific Research/Earth and Life).

Submitted: 14 June 2005
Accepted: 28 October 2005

References

Apel, E.D., R.M. Lewis, R.M. Grady, and J.R. Sanes. 2000. Syne-1, a dystrophin- and Klarsicht-related protein associated with synaptic nuclei at the neuromuscular junction. *J. Biol. Chem.* 275:31986–31995.

Borradori, L., and A. Sonnenberg. 1999. Structure and function of hemidesmosomes: more than simple adhesion complexes. *J. Invest. Dermatol.* 112:411–418.

Brummelkamp, T.R., R. Bernards, and R. Agami. 2002. A system for stable expression of short interfering RNAs in mammalian cells. *Science.* 296:550–553.

Burke, B., and C.L. Stewart. 2002. Life at the edge: the nuclear envelope and human disease. *Nat. Rev. Mol. Cell Biol.* 3:575–585.

de Pereda, J.M., G. Wiche, and R.C. Liddington. 1999. Crystal structure of a tandem pair of fibronectin type III domains from the cytoplasmic tail of integrin alpha6beta4. *EMBO J.* 18:4087–4095.

Fuchs, E., and I. Karakesisoglou. 2001. Bridging cytoskeletal intersections. *Genes Dev.* 15:1–14.

Fuchs, P., M. Zorer, G.A. Rezniczek, D. Spazierer, S. Oehler, M.J. Castanon, R. Hauptmann, and G. Wiche. 1999. Unusual 5′ transcript complexity of plectin isoforms: novel tissue-specific exons modulate actin binding activity. *Hum. Mol. Genet.* 8:2461–2472.

Geerts, D., L. Fontao, M.G. Nievers, R.Q. Schaapveld, P.E. Purkis, G.N. Wheeler, E.B. Lane, I.M. Leigh, and A. Sonnenberg. 1999. Binding of integrin α6β4 to plectin prevents plectin association with F-actin but does not interfere with intermediate filament binding. *J. Cell Biol.* 147:417–434.

Grady, R.M., D.A. Starr, G.L. Ackerman, J.R. Sanes, and M. Han. 2005. Syne proteins anchor muscle nuclei at the neuromuscular junction. *Proc. Natl. Acad. Sci. USA.* 102:4359–4364.

Gruenbaum, Y., A. Margalit, R.D. Goldman, D.K. Shumaker, and K.L. Wilson. 2005. The nuclear lamina comes of age. *Nat. Rev. Mol. Cell Biol.* 6:21–31.

Guo, L., L. Degenstein, J. Dowling, Q.C. Yu, R. Wollmann, B. Perman, and E. Fuchs. 1995. Gene targeting of BPAG1: abnormalities in mechanical strength and cell migration in stratified epithelia and neurologic degeneration. *Cell.* 81:233–243.

Guttman, J.A., D.J. Mulholland, and A.W. Vogl. 1999. Plectin is concentrated at intercellular junctions and at the nuclear surface in morphologically differentiated rat Sertoli cells. *Anat. Rec.* 254:418–428.

Hieda, Y., Y. Nishizawa, J. Uematsu, and K. Owaribe. 1992. Identification of a new hemidesmosomal protein, HD1: a major, high molecular mass component of isolated hemidesmosomes. *J. Cell Biol.* 116:1497–1506.

Hopkinson, S.B., and J.C.R. Jones. 2000. The N terminus of the transmembrane protein BP180 interacts with the N-terminal domain of BP230, thereby mediating keratin cytoskeleton anchorage to the cell surface at the site of the hemidesmosome. *Mol. Biol. Cell.* 11:277–286.

Hutchison, C.J. 2002. Lamins: building blocks or regulators of gene expression? *Nat. Rev. Mol. Cell Biol.* 3:848–858.

Ingber, D.E. 2003a. Tensegrity I. Cell structure and hierarchical systems biology. *J. Cell Sci.* 116:1157–1173.

Ingber, D.E. 2003b. Tensegrity II. How structural networks influence cellular information processing networks. *J. Cell Sci.* 116:1397–1408.

Jefferson, J.J., C.L. Leung, and R.K. Liem. 2004. Plakins: goliaths that link cell junctions and the cytoskeleton. *Nat. Rev. Mol. Cell Biol.* 5:542–553.

Kakinuma, T., H. Ichikawa, Y. Tsukada, T. Nakamura, and B.H. Toh. 2004. Interaction between p230 and MACF1 is associated with transport of a glycosyl phosphatidyl inositol-anchored protein from the Golgi to the cell periphery. *Exp. Cell Res.* 298:388–398.

Karakesisoglou, I., Y. Yang, and E. Fuchs. 2000. An epidermal plakin that integrates actin and microtubule networks at cellular junctions. *J. Cell Biol.* 149:195–208.

Koster, J., D. Geerts, B. Favre, L. Borradori, and A. Sonnenberg. 2003. Analysis of the interactions between BP180, BP230, plectin and the integrin alpha6beta4 important for hemidesmosome assembly. *J. Cell Sci.* 116:387–399.

Koster, J., L. Borradori, and A. Sonnenberg. 2004a. Hemidesmosomes: Molecular organization and their importance for cell adhesion and disease. *In* Cell Adhesion. J. Behrens and W.J. Nelson, editors. Springer-Verlag New York Inc., New York. 243–280.

Koster, J., S. van Wilpe, I. Kuikman, S.H. Litjens, and A. Sonnenberg. 2004b. Role of binding of plectin to the integrin beta4 subunit in the assembly of hemidesmosomes. *Mol. Biol. Cell.* 15:1211–1223.

Leung, C.L., M. Zheng, S.M. Prater, and R.K. Liem. 2001. The BPAG1 locus: alternative splicing produces multiple isoforms with distinct cytoskeletal linker domains, including predominant isoforms in neurons and muscles. *J. Cell Biol.* 154:691–697.

Libotte, T., H. Zaim, S. Abraham, V.C. Padmakumar, M. Schneider, W. Lu, M. Munck, C. Hutchison, M. Wehnert, B. Fahrenkrog, et al. 2005. Lamin A/C-dependent localization of Nesprin-2, a giant scaffolder at the nuclear envelope. *Mol. Biol. Cell*. 16:3411–3424.

Lin, C.M., H.J. Chen, C.L. Leung, D.A. Parry, and R.K. Liem. 2005. Microtubule actin crosslinking factor 1b: a novel plakin that localizes to the Golgi complex. *J. Cell Sci.* 118:3727–3738.

Litjens, S.H., J. Koster, I. Kuikman, S. van Wilpe, J.M. de Pereda, and A. Sonnenberg. 2003. Specificity of binding of the plectin actin-binding domain to beta4 integrin. *Mol. Biol. Cell.* 14:4039–4050.

Maniotis, A.J., C.S. Chen, and D.E. Ingber. 1997. Demonstration of mechanical connections between integrins, cytoskeletal filaments, and nucleoplasm that stabilize nuclear structure. *Proc. Natl. Acad. Sci. USA*. 94:849–854.

Mislow, J.M., M.S. Kim, D.B. Davis, and E.M. McNally. 2002. Myne-1, a spectrin repeat transmembrane protein of the myocyte inner nuclear membrane, interacts with lamin A/C. *J. Cell Sci*. 115:61–70.

Mosley-Bishop, K.L., Q. Li, L. Patterson, and J.A. Fischer. 1999. Molecular analysis of the klarsicht gene and its role in nuclear migration within differentiating cells of the *Drosophila* eye. *Curr. Biol.* 9:1211–1220.

Nakayama, M., R. Kikuno, and O. Ohara. 2002. Protein-protein interactions between large proteins: two-hybrid screening using a functionally classified library composed of long cDNAs. *Genome Res.* 12:1773–1784.

Padmakumar, V.C., S. Abraham, S. Braune, A.A. Noegel, B. Tunggal, I. Karakesisoglou, and E. Korenbaum. 2004. Enaptin, a giant actin-binding protein, is an element of the nuclear membrane and the actin cytoskeleton. *Exp. Cell Res.* 295:330–339.

Rezniczek, G.A., C. Abrahamsberg, P. Fuchs, D. Spazierer, and G. Wiche. 2003. Plectin 5′-transcript diversity: short alternative sequences determine stability of gene products, initiation of translation and subcellular localization of isoforms. *Hum. Mol. Genet.* 12:3181–3194.

Schaapveld, R.Q., L. Borradori, D. Geerts, M.R. van Leusden, I. Kuikman, M.G. Nievers, C.M. Niessen, R.D. Steenbergen, P.J. Snijders, and A. Sonnenberg. 1998. Hemidesmosome formation is initiated by the β4 integrin subunit, requires complex formation of β4 and HD1/plectin, and involves a direct interaction between β4 and the bullous pemphigoid antigen 180. *J. Cell Biol.* 142:271–284.

Seed, B., and A. Aruffo. 1987. Molecular cloning of the CD2 antigen, the T-cell erythrocyte receptor, by a rapid immunoselection procedure. *Proc. Natl. Acad. Sci. USA.* 84:3365–3369.

Spann, T.P., R.D. Moir, A.E. Goldman, R. Stick, and R.D. Goldman. 1997. Disruption of nuclear lamin organization alters the distribution of replication factors and inhibits DNA synthesis. *J. Cell Biol.* 136:1201–1212.

Spann, T.P., A.E. Goldman, C. Wang, S. Huang, and R.D. Goldman. 2002. Alteration of nuclear lamin organization inhibits RNA polymerase II–dependent transcription. *J. Cell Biol.* 156:603–608.

Starr, D.A., and M. Han. 2002. Role of ANC-1 in tethering nuclei to the actin cytoskeleton. *Science.* 298:406–409.

Starr, D.A., and M. Han. 2003. ANChors away: an actin based mechanism of nuclear positioning. *J. Cell Sci.* 116:211–216.

Starr, D.A., G.J. Hermann, C.J. Malone, W. Fixsen, J.R. Priess, H.R. Horvitz, and M. Han. 2001. Unc-83 encodes a novel component of the nuclear envelope and is essential for proper nuclear migration. *Development.* 128:5039–5050.

Sterk, L.M., C.A. Geuijen, L.C. Oomen, J. Calafat, H. Janssen, and A. Sonnenberg. 2000. The tetraspan molecule CD151, a novel constituent of hemidesmosomes, associates with the integrin α6β4 and may regulate the spatial organization of hemidesmosomes. *J. Cell Biol.* 149:969–982.

Sun, D., C.L. Leung, and R.K. Liem. 2001. Characterization of the microtubule binding domain of microtubule actin crosslinking factor (MACF): identification of a novel group of microtubule associated proteins. *J. Cell Sci.* 114:161–172.

van Ham, S.M., E.P. Tjin, B.F. Lillemeier, U. Gruneberg, K.E. van Meijgaarden, L. Pastoors, D. Verwoerd, A. Tulp, B. Canas, D. Rahman, et al. 1997. HLA-DO is a negative modulator of HLA-DM-mediated MHC class II peptide loading. *Curr. Biol.* 7:950–957.

Wiche, G. 1998. Role of plectin in cytoskeleton organization and dynamics. *J. Cell Sci.* 111:2477–2486.

Wilhelmsen, K., S. Burkhalter, and P. van der Geer. 2002. C-Cbl binds the CSF-1 receptor at tyrosine 973, a novel phosphorylation site in the receptor's carboxy-terminus. *Oncogene.* 21:1079–1089.

Yan, Y., E. Winograd, A. Viel, T. Cronin, S.C. Harrison, and D. Branton. 1993. Crystal structure of the repetitive segments of spectrin. *Science.* 262:2027–2030.

Zhang, Q., J.N. Skepper, F. Yang, J.D. Davies, L. Hegyi, R.G. Roberts, P.L. Weissberg, J.A. Ellis, and C.M. Shanahan. 2001. Nesprins: a novel family of spectrin-repeat-containing proteins that localize to the nuclear membrane in multiple tissues. *J. Cell Sci.* 114:4485–4498.

Zhang, Q., C. Ragnauth, M.J. Greener, C.M. Shanahan, and R.G. Roberts. 2002. The nesprins are giant actin-binding proteins, orthologous to *Drosophila melanogaster* muscle protein MSP-300. *Genomics.* 80:473–481.

Zhen, Y.Y., T. Libotte, M. Munck, A.A. Noegel, and E. Korenbaum. 2002. NUANCE, a giant protein connecting the nucleus and actin cytoskeleton. *J. Cell Sci.* 115:3207–3222.